MATHEMATICAL MODELING AND COMPUTING, Vol. 8, No. 2, pp. 304–316 (2021)

Mitigating geolocation errors in nighttime light satellite data and global CO_2 emission gridded data

Kinakh V.[1], Oda T.[2,3,4], Bun R.[1,5], Novitska O.[1]

[1] *Lviv Polytechnic National University, 12 S. Bandera Str., 79013, Lviv, Ukraine*
[2] *Universities Space Research Association, Columbia, MD, USA*
[3] *University of Maryland, College Park, MD, USA*
[4] *Osaka University, Suita, Osaka, Japan*
[5] *WSB University, Dąbrowa Górnicza, Poland*

(Received 5 March 2021; Accepted 10 May 2021)

Accurate geospatial modeling of greenhouse gas (GHG) emissions is an essential part of the future of global GHG monitoring systems. Our previous work found a systematic displacement in the high-resolution carbon dioxide (CO_2) emission raster data of the Open-source Data Inventory for Anthropogenic CO_2 (ODIAC) emission product. It turns out this displacement is due to geolocation bias in the Defense Meteorological Satellite Program (DMSP) nighttime lights (NTL) data products, which are used as a spatial emission proxy for estimating non-point source emissions distributions in ODIAC. Mitigating such geolocation error (~ 1.7 km), which is on the same order of the size of the carbon observing satellites field of view, is especially critical for the spatial analysis of emissions from cities. In this paper, there is proposed a method to mitigate the geolocation bias in DMSP NTL data that can be applied to DMSP NTL-based geospatial products, such as ODIAC. To identify and characterize the geolocation bias, we used the OpenStreetMap repository to define city boundaries for a large number of global cities. Assumption is that the total emissions within the city boundaries are at the maximum if there is no displacement (geolocation bias) in NTL data. Therefore, it is necessary to find an optimal vector (distance and angle) that maximizes the ODIAC total emissions within cities by shifting the emission fields. In the process of preparing annual composites of the nighttime stable lights data, some pixels of the DMSP data corresponding to water bodies were zeroed, which due to the geolocation bias unreasonably distorted the ODIAC emission fields. Hence, an original approach for restoring data in such pixels is considered using elimination of the factor that distorted the ODIAC emission fields. It is also proposed a bias correction method for shifted high-resolution emission fields in ODIAC. The bias correction was applied to multiple cities from the different continents. It is shown that the bias correction to the emission data (elimination of geolocation error in non-point emission source fields) increases the total CO_2 emissions within city boundaries by 4.76% on average, due to reduced emissions from non-urban areas to which these emissions were likely to be erroneously attributed.

Keywords: *remote sensing, nighttime lights data, greenhouse gas emission, satellite data bias, bias analysis algorithm.*

2010 MSC: 91B76, 65G99 **DOI:** 10.23939/mmc2021.02.304

1. Introduction

Satellite remote sensing data are widely used to analyze many processes of human activity [1–4]. In particular, remote sensing data on nighttime light intensity from Defense Meteorological Satellite Program (DSMP) satellites [5–7], due to unique long record, are used as a proxy to model many human activities and natural processes [8–11]. In an original way these data are also used to create the Open-source Data Inventory for Anthropogenic CO_2 (ODIAC) high-resolution raster data (30×30 arc

seconds or approximately 1×1 km at the equator) on carbon dioxide (CO_2) emissions from fossil fuel consumption for energy purposes [12–14]. The ODIAC high-resolution maps are based on emission data from point sources and disaggregation of country-level CO_2 emissions data from non-point sources using nightlight data. The emissions values distribution depends on the intensity of nightlight data, taking into account the other factors [12].

ODIAC global data are widely used to estimate CO_2 emissions from many regions of our planet [15–17]. However, when analyzing ODIAC data for urban areas, we noticed a displacement of the data (to be precise, the DSMP nightlight data that underlies them) in relation to real objects (see [18]). The bias in the high-resolution raster data is visually noticeable for emissions data for many cities from all continents, but it is best seen for small cities without neighboring settlements.

For example, Fig. 1 illustrates the shift/displacement of city emissions seen in the ODIAC raster data on CO_2 emissions for three global cities: Warsaw, Poland; New York, US; and Armidale, Australia. Compared to the city boundaries, city emissions indicated by the ODIAC data seem to be shifted towards the northwest direction. Warsaw, Poland (Fig. 1a) was particularly interesting to examine, because of the Vistula River, which flows in the middle of the city towards the northwest direction (it is parallel to the direction of the NTL bias). New York City (Fig. 1b) was also interesting to examine, because of Hudson River (the width is commensurate with the DMSP/ODIAC data cell size), which flows in parallel to the intensively built-up Manhattan area, but perpendicular to the NTL geolocation bias. In contrast, Armidale, Australia is not a big city (population is 26 500) and there are no neighboring settlements with intensive nighttime lights.

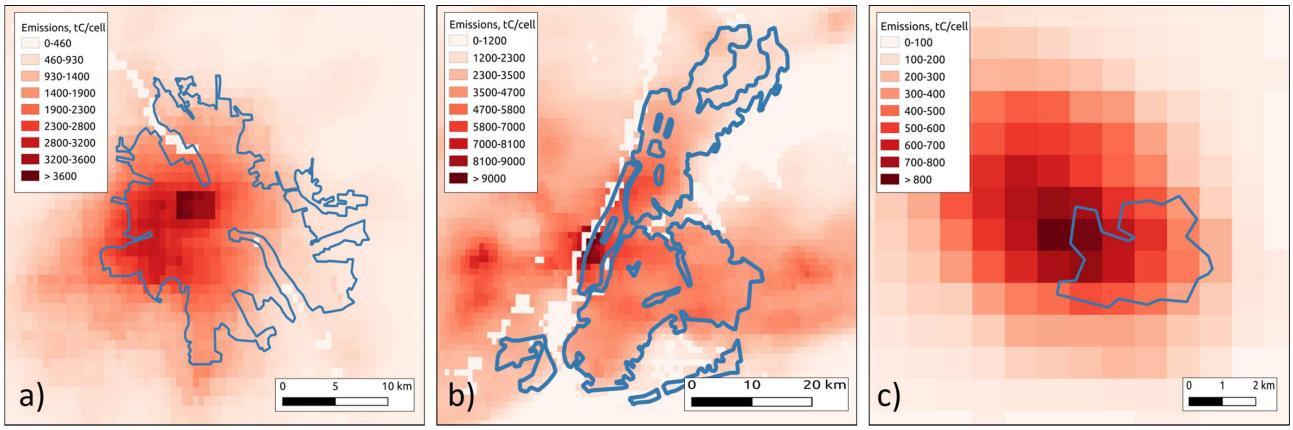

Fig. 1. Examples of cities from the different continents for illustration of geolocation biases in ODIAC emission data (inherited from DMSP nighttime light data): Warsaw, Poland (a); New York, US (b); and Armidale, Australia (c). ODIAC2014 emission data from non-point sources (emissions for 2014) on 30 arc seconds grid are calculated basing on DMSP'2010/2011 data (see [13]). Blue polygons indicate city boundaries, according to OpenStreetMap (OSM) data [19].

The displacement in ODIAC/DMSP raster data was also found when comparing this data with the other high-resolution greenhouse gas data for Poland, which have been calculated using a so-called "bottom-up" approach — Geoinformation technologies, spatio-temporal approaches, and full carbon account for improving the accuracy of GHG inventories (GESAPU) [18, 20, 21]. Even if the geolocation error is small (~ 1.7 km), it can significantly distort the emission values within cities or urban areas [15, 22, 23]. It is also important to note that the magnitude of geolocation biases is on the same order of the size as the satellite footprints of the recent carbon observing satellites, such as OCO-2 [24] and OCO-3 [25]. This means that the geolocation errors are large enough to impact the analysis of city emissions using satellite data.

The specified ODIAC raster data bias was inherited from DMSP data. ODIAC directly uses the DMSP data to distribute non-point source emissions (see [12, 13]). The use of the DMSP data for geospatial modeling applications has been actively examined. In particular, there are publications

devoted to analyzing specific effects and improving the parameters of these data (for example, the effects of saturation, blooming, diffusion, etc. [26–30]). However, the bias of these data in relation to real light sources has been not fully examined. Therefore, this study aimed to estimate the bias vector (magnitude and direction of the bias) of ODIAC raster data inherited by the primary nightlight data and to investigate which parameters or factors this bias depends on. We present methodology, a mathematical apparatus, and algorithm for estimating the bias vectors of the ODIAC raster data on CO_2 emissions, using city boundaries from the open-source repository OpenStreetMap (OSM [19]). After the bias vector estimation, our method is applied to compensate the geolocation error in ODIAC high-resolution emissions and to improve city emissions estimations. As a result, a corresponding algorithm for correcting the displacement of the initial raster data is presented. We demonstrate the main stages of algorithm application for estimating displacement and compensation on a number of cities from the different continents.

2. Methods

There are a few approaches to improve a number of parameters of high-resolution DMSP data on nighttime lights, including geolocation error [31–33]. In this paper, it is presented an original approach to estimating and compensating for geolocation error of ODIAC data on CO_2 emissions (the error inherited from DMSP data), which is based on data on city boundaries and water bodies. This approach is a further improvement of a previously described approach [34]. It includes steps to estimate the bias and computational procedures to compensate for this bias and reduce the geolocation error.

2.1. Bias calculation

The idea of the proposed method for bias vector search presumes that the total value of ODIAC CO_2 emissions from non-point sources within the city boundaries should be at the maximum if the primary remote sensing nightlight data (DMSP data) are correctly positioned without any geolocation error. There is no bias in the nighttime lights remote sensing data if this condition is satisfied. Moreover, any shift in nightlight data leads to the decrease in the total ODIAC CO_2 emission value within the cities. It can serve as an indicator of the bias in nighttime lights data. This assumption may not be true for a separate city because of various reasons: industrial zone located outside of the city; neighboring settlements and so on. However, this assumption is true for total emissions from a large number of the cities.

In the analysis of the biases of nightlight raster data, there are used two methods based on the calculation of the total emissions within vector polygons of:

— city boundaries from the open-source repository OSM [19];
— the set of city boundaries from OSM within a vector grid with cells of size $1^\circ \times 1^\circ$ latitude and longitude.

36 432 cities from the OSM city boundaries database (the first method), and 2 237 cells with cities (the second method) have been analyzed. To find a bias vector (distance and direction) for a separate city, it would be necessary to shift the ODIAC raster data pixels with emission values by a certain distance and angle, then iteratively calculate total emissions within the city and find such a bias vector (distance and direction), which provides maximum value of emissions (Fig. 2a). But the emission values are represented by raster data with a fixed global regular grid and a pixel size of 30 arc-seconds. Therefore, in computational experiments it is much easier to shift city boundaries as vector objects in the opposite direction and iteratively search for the optimal bias vector, which provides the maximum total emissions within cities boundaries (Fig. 2b).

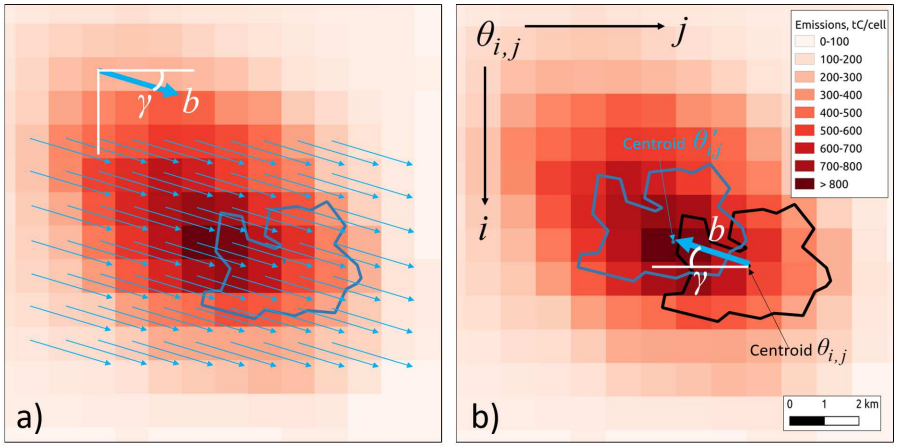

Fig. 2. The proposed bias search method illustrated for the city of Armidale, Australia. The ODIAC2014 dataset is used (ODIAC emissions from non-point sources for 2014 are calculated based on DMSP'2010/2011 data, see [13]). In case there is a bias in the nightlight data in relation to the real objects, the first idea is to shift all pixels of the data for some distance and for some angle to get the maximal emission value within the given city boundary (a). The second idea is to shift a city boundary polygon in the opposite direction that provides the maximum emissions within the city boundary (b).

To find the optimal bias vector (distance and direction), moving city boundaries is an optimization task (Fig. 3). Let $\theta_{i,j}$ be the pixel of the ODIAC emission raster data with coordinates i and j, and its value $e_{i,j}$ are the total emissions within this pixel. Let P_{city} be the polygon of analyzed city boundary, and P'_{city} be the polygon of this city shifted by distance b in direction γ. The total emissions within the polygon P'_{city} can be calculated using the formula:

$$E_{city}(b,\gamma) = \sum_{\forall \theta_{i,j} \cap P'_{city}(b,\gamma)} e_{i,j},$$

where $\cap$ is the operation of intersection (common territory) of two geographical objects. Emissions from the incomplete pixels of the intersection are calculated in proportion to the common area. The task to find the optimal bias means the task of finding such values of distance (b_{opt}) and angle (γ_{opt}) that provide the maximum total emissions within the city boundaries:

$$\max_{b\in[0;b_{max}],\gamma\in[0,360]} [E_{city}(b,\gamma)] \to E_{city,max}(b_{opt},\gamma_{opt}).$$

It is assumed that the function $E_{city}(b,\gamma)$ is continuous because a vector map of city boundaries was used and emissions of pixels being partially within the city boundaries were calculated (sampled) in proportion to the intersection. In the process of calculation of correction vector, its direction was opposite to the found bias vector, so it showed how much and at what angle was necessary to shift the ODIAC raster emissions data to compensate for the geolocation error of nighttime light data.

The algorithm for bias vector calculation is iterative one. In the beginning, the city boundary was shifted in eight directions (east, southeast, south, etc.) with a given step of 0.01° (it is approximately 1.1 km at the equator), and then eight values of total emissions within the new shifted city boundaries were calculated. We identified the city boundary centroid, which corresponds to the maximum value of the total emissions, and then shifted the initial city boundary centroid to this point. Then, the step size was halved, and the same operations were realized: shifting in eight directions, emissions calculation, finding direction with maximum emissions, and shifting the city boundary to the point with maximum emissions. After eight such iterations of step size halving, it was equal to $0.01°/2^8$ (which is close to 4 meters at the equator, and it decreases with increasing latitude; for example, for the latitude of Ukraine this step is approximately 2 m in the horizontal direction) and thus the optimal bias vector was found.

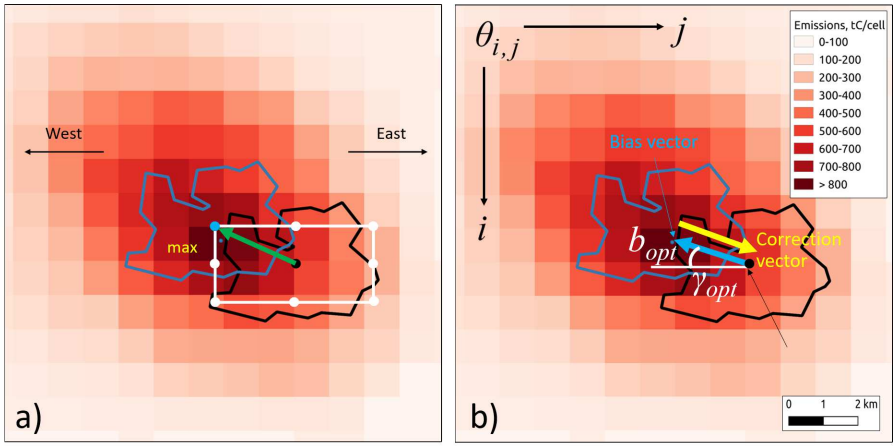

Fig. 3. Illustration of the algorithm for bias calculation (Armidale, Australia as an example). In the first step (a) the city boundary polygon is shifted by 0.01° in eight directions, each time calculating the emissions within the city. Next, we chose as a basis the bias variant that provided maximum emissions, reduced the step size by half, and again shifted the polygon in eight directions. After eight such iterations of step size reduction, we obtained the desired bias vector ($\overline{b}$).

It was shown in our previous work [34] that the proposed algorithm well determines the bias in the horizontal and vertical directions, which is translated into the bias length and angle. Using this approach, one can find the correction vector (opposite to bias vector), that shows how far and in what direction it is necessary to shift the emission data, so the total emission within the city boundaries is at the maximum. It was shown in [34] that this geolocation error depends on latitude, and the corresponding formulas are established, by virtue of which the correction vectors can be calculated to compensate for the bias.

2.2. Geolocation bias and water objects

Preparing annual composites of nighttime lights data, the DMSP team used a procedure of "cleaning" the remote sensing data from the background noise in which a zero value of light intensity was assigned to some pixels [7]: areas that correspond to large rivers, lakes, seas, or oceans, according to landcover maps. But the ODIAC non-point source emission fields were built using these cleaned DMSP data. Therefore, considering the bias of nightlight data, the "cleaning" procedure may assign zero values to pixels with nonzero emissions in reality. When calculating the total greenhouse gas emissions within the city boundaries, the values of such "cleaned" pixels can influence the results. For example, it is shown in Fig. 1b that the maximum of emissions corresponding to Manhattan was shifted towards the Hudson River due to the bias in nighttime lights data, and then some cells were additionally filled with zero as for the water objects. With the aim to compensate for the geolocation error, we should shift these zero data towards Manhattan, that doesn't correspond to reality. Therefore, before the bias compensation, it is necessary to "restore" the data in such "cleaned" pixels. There are proposed two methods of operating with such pixels within the water objects:

— for the small water objects within high emission areas (for example, rivers or lakes within the cities) there is applied the second-order polynomial interpolation using pixel values around the target pixel;
— for the large water objects (coastal areas, big lakes, etc.) there is applied the second-order interpolation polynomial built on pixel values from the coast side (the pixels were used from the opposite direction to the bias) and extrapolated emissions for "cleaned" pixels.

Because the DMSP data bias is in the northwest direction, according to the first method mentioned above, we moved horizontally along the rows of the ODIAC data raster and selected zero cells that

had at least three non-zero neighboring cells on each side. Based on the emissions of these cells, we created two second-order interpolation functions on each side, approximated using them the two emission values in the target cell, and then calculated the average value.

Again, since the DMSP data bias is in the northwest direction, the second method deals with zero cells, which also have neighboring zero cells on the left and at least three non-zero cells on the right. Based on these non-zero cells, there is constructed the second-order interpolation polynomial to approximate the emission value in the target cell. This method allowed us to deal with the emission values for biased cells on the western coastal lines of seas, lakes, and other large water bodies.

Fig. 4, illustrates the proposed methods of dealing with zero value cells on the examples of Warsaw, Poland and New York, US. According to the formulas given in Kinakh et al. [34], the bias of the ODIAC emission data (inherited from the DMSP bias of nighttime lights data) is 1 659 meters (at an angle of 27.4° in the northwest direction) for Warsaw, and 1 762 meters (also at an angle of 27.4°) for New York.

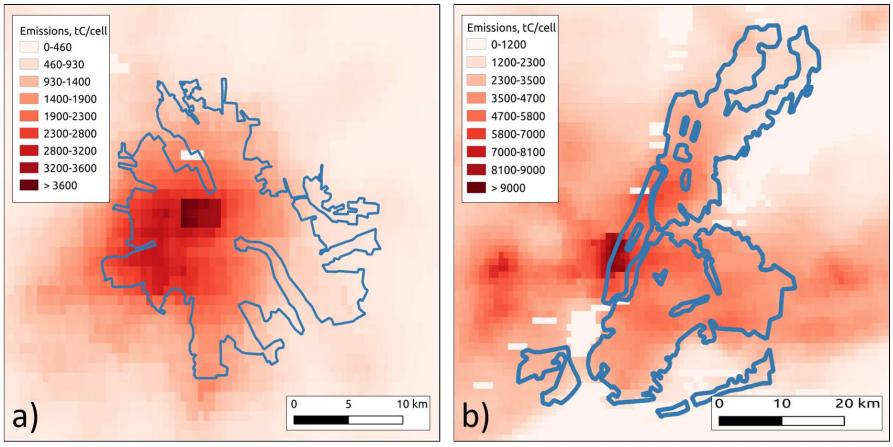

Fig. 4. Illustration of dealing with the ODIAC biased data on emissions from non-point sources, which due to the bias of the DMSP data on nighttime lights were occurred in the cells covering the water bodies and were "cleaned" in the process of preparation of annual composites of stable lights. In particular, the data are shown at the location of the Vistula River in Warsaw, Poland (a) and Hudson River in New York, US (b).

3. Results: geolocation bias mitigation

The bias vector can be estimated for any geographical area using the approach described above. Therefore, the next step was to compensate emission data for the spatial displacement. The first idea was to shift ODIAC emissions data by the estimated compensation vector. But the compensation procedure could not consist of shifting ODIAC pixels by a certain distance and angle as the data should be presented using a 30 arc-second regular grid. Consequently, there is proposed the next compensation algorithm. The compensation for the cell $\theta_{i,j}$ should consist of the following steps (Fig. 5):

— shifting the cell $\theta_{i,j}$, where i and j are its coordinates, to the bias direction for the distance b_{opt} with angle γ_{opt} ($\theta'_{i,j}$ is the shifted cell);
— calculating the sum of emissions $e(\theta_{i,j}) = \sum_{k,l;\forall\theta'_{i,j}\cap\theta_{k,l}} e^{'}(\theta_{k,l})$ as parts $e^{'}(\theta_{k,l})$ of corresponding cells values, crossed by the shifted pixel (in proportions to the overlapped area between each cell and shifted cell), where $\cap$ is the intersection operation between two geographical objects: cells $\theta'(i,j)$ and $\theta(k,l)$;
— saving the results as the corrected emissions for the initial cell $\theta(i,j)$.

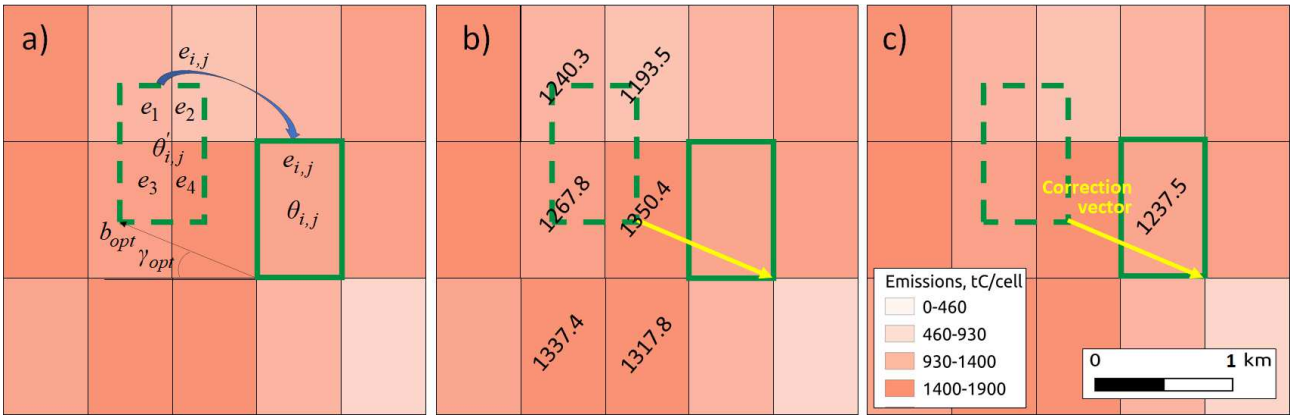

Fig. 5. Illustration of the compensation algorithm (a); examples of input pixels that take part in calculations and their values (b); calculated pixels and their values (c) (fragment of ODIAC emissions from non-point sources for Warsaw, Poland).

Examples of cells of ODIAC gridded emission data that take part in these procedures (compensation of bias) and their values for Warsaw emissions are presented in Fig. 5b, while compensated cells and their values are illustrated in Fig. 5c. The described procedures enable to mitigate the emission data that fell into the water bodies due to the DMSP data bias, and compensate for the bias. Presented in Fig. 6 are examples of emission data for several cities; we show data in which the geolocation error caused by the DMSP data was compensated.

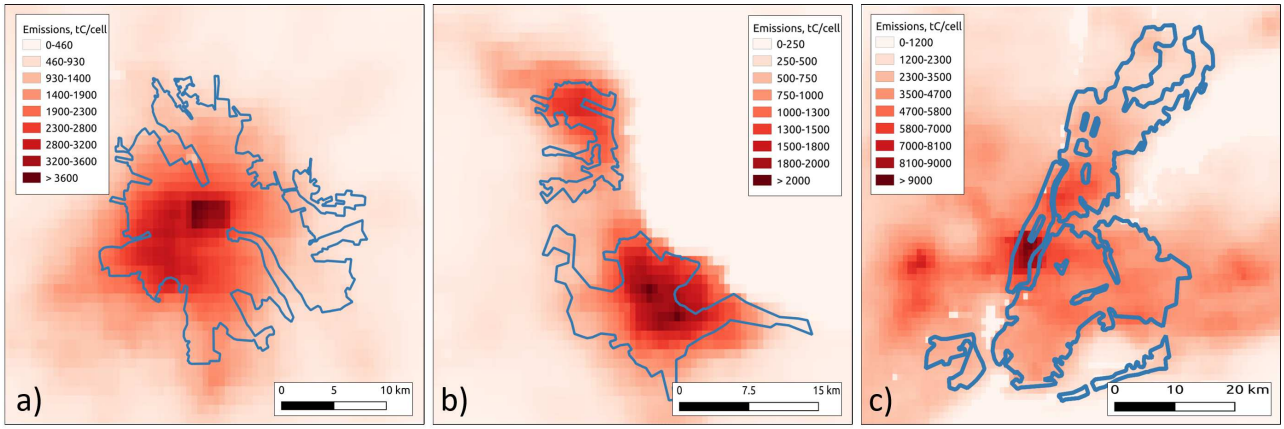

Fig. 6. The illustration of ODIAC'2014 emission data from non-point sources with compensated bias inherited from DMSP data on the following: Warsaw, Poland (a); Gdynia and Gdansk, Poland (b); and New York, USA (c).

The emission data described above, obtained from the bias compensation, are much better because the geolocation error was minimized. However, these data may consist of non-zero emission values at the sites of water and other objects, which were cleaned/assigned with zero values of nighttime lights when preparing annual composites of the DMSP data. Therefore, at the final stage of the ODIAC data bias compensation, the emission data should be filled with zero values in cells corresponding to these objects. To fill such cells with zeros, we extracted the mask of cells with zero values from the initial data, and then use the mask for filling in zeros for corresponding cells in the resulting raster. As a result of this operation, we obtained an adjusted raster of the ODIAC emission data (Fig. 7), which completely corresponds to the input raster for cells with zero and non-zero emissions, but with compensated bias caused by the geolocation error of the DMSP nighttime lights data.

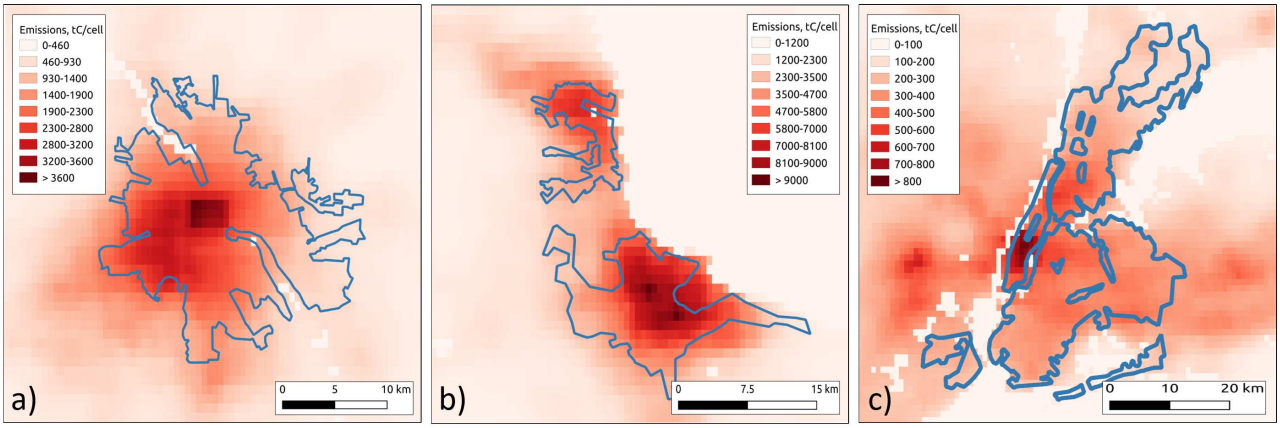

Fig. 7. Examples of ODIAC emission data from non-point sources with compensated bias and recovered zero value mask within the water and other objects: Warsaw, Poland (a); Gdynia and Gdansk, Poland (b); and New York, USA (c).

Table 1 presents the results of implementing our approach to compensate for bias of the ODIAC emission data (bias which was inherited from the DMSP data bias) at the level of total emissions from non-point sources from the country's cities (US cities were additionally split into four parts to better consider the specificity of the DMSP data bias). For all the countries analyzed, eliminating the geolocation error led to an increase in total emissions from non-point sources within cities, and this was due to a decrease in emissions from non-urban areas.

Table 1. Results of compensation of the bias of the ODIAC'2014 emission data at the country level: total emissions from non-point sources within cities under analysis (city boundaries from OSM repository).

Country	Number of cities under analysis	Total emissions with bias, tC	Bias: Longitude direction, degree	Bias: Latitude direction, degree	Bias distance, m	Bias angle to Western direction, degree	Total emissions (after bias compen-sation), tC	Emission increase, %
Brazil	844	17 584 358	-0.0126	0.0032	1 386	14.88	18 223 439	3.63
China	1 471	126 300 508	-0.0087	0.0112	1 474	58.03	133 009 431	5.31
France	630	6 712 919	-0.0209	0.0078	1 817	28.53	7 108 942	5.90
Germany	2 207	15 717 867	-0.0208	0.0025	1,817	10.86	16 496 187	4.95
India	950	26 683 982	-0.0156	0.0101	1 968	34.68	28 886 771	8.26
Italy	255	1 862 212	-0.0200	0.0058	1 778	21.18	1 993 781	7.07
Japan	508	10 074 234	-0.0165	0.0116	1 932	41.69	11 278 865	11.96
Poland	891	6 085 082	-0.0216	0.0070	1 667	27.94	6 491 137	6.67
South Africa	151	6 114 083	-0.0134	-0.0040	1,377	-18.76	6 260 143	2.39
Spain	309	3 675 575	-0.0155	0.0098	1 718	39.55	4,051,115	10.22
Ukraine	2 491	8 404 550	-0.0209	0.0064	1 702	24.72	8 979 201	6.84
US, bottom left part [1]	688	26 958 833	-0.0159	0.0035	1 589	14.24	27 540 459	2.16
US, bottom right part	2 811	56 686 725	-0.0131	0.0074	1 488	33.65	58 597 494	3.37
US, top left part	765	8 949 422	-0.0131	0.0078	1 374	39.19	9 386 657	4.89
US, top right part	2 907	84 180 755	-0.0186	0.0084	1 374	33.56	87 005 027	3.36

[1]To split US emissions to bottom and top parts we used 39° N, and to left and right part we used 99° W.

4. Discussion and conclusions

The high-resolution ODIAC data on CO_2 emissions from non-point sources have a bias that is inherited from the bias of the DMSP data on nighttime lights. There is no analysis of the physical nature of this bias in the paper, but there are studied the possibilities of reducing the geolocation error of non-point emission sources caused by such a bias. The presented approach makes it possible to find the magnitude and direction of the bias, recover the data distorted due to the overlap of biased emission data on water and other zero-emission objects, compensate for the bias, and present the emission data on a regular grid. The approach uses the boundaries of a large number of cities from the OSM repository. It can't be applied to a separate city, because in this case, undesirable disturbing factors can play a significant role, such as the presence of suburban industrial zones, neighboring settlements with significant emissions, and large zero-emission zones within the city (park or river) and neighborhood (sea, forest, etc.). Such perturbing factors make it impossible to correctly identify the distance and direction of the bias, but in the case of a large number of cities under analysis, these factors are mutually compensated.

As calculations [34] have shown, the bias distance of the ODIAC/DMSP data is about $1\,600 - 1\,800$ meters and is weakly dependent on other parameters. The direction of the bias is northwestern, the angle varies mainly in the range of $7^\circ - 32^\circ$ in relation to the western direction, and this angle depends significantly on latitude. The perturbing factors, to some extent, affect the results of calculations, as seen in Table 1. In countries with a large number of analyzed cities, the distance and direction of the bias correspond to the values given in Kinakh et al. [34]. But, in South Africa, for example, the bias distance, and especially its direction, deviate from the general rule. The main factors that influenced this result are the smaller number of cities under analysis, the big cities are mostly located close to large zero-emission territories (the ocean), and the country is located at high latitudes in the southern hemisphere. In general, the impact of a long coastline is more noticeable in countries where a significant part of the coastline is perpendicular to the direction of the DMSP data bias (Italy, Japan, parts of the US), and less noticeable when a significant part of the coastline is parallel to the DMSP data bias (e.g., Poland, Ukraine).

The above results on the identification of emission data bias and its compensation were calculated for the ODIAC emission data for 2014 (they were obtained on the basis of the DMSP data for 2010 and 2011 as a spatial proxy [12], and therefore they inherited the bias of these data). The question arises: what is the bias of other DMSP data on nighttime lights? A detailed analysis of the DMSP data bias for other years and different DMSP satellites using many cities from all continents is beyond the scope of the current study. But as an example, Fig. 8 presents the results of a study on the bias of the DMSP data on nighttime lights using the approach based on the analysis of 653 biggest cities of Ukraine. The study covered all available uncalibrated nighttime lights monitoring data from all DMSP satellites [7]. In the figure, the monitoring data (annual composites) from different satellites are highlighted in different colors. As we see, the data from the satellites F12, F14, F15, and F16 in the first years of their operation had a fairly low bias magnitude, which did not exceed 600 meters. For F15 satellite data for 2000, the lowest bias value was observed (82 meters). Although for this satellite, the largest observed bias value was in 2008 and 2007.

It can be concluded that if more than one satellite is available for a given year, it is possible to select data with a smaller bias. For example, the 1994 F12 satellite data have a smaller bias than F10 data, the 2002 F14 satellite data have a smaller bias than F15, and in 2008 there was a moderate bias for the F16 satellite data as opposed to the maximum observed bias for F15 data. Also, from Fig. 8, one can notice that the satellites' data's accuracy worsens in the last years of operation. The bias angle, in most cases is close to 30° in the northwest direction. It is worth noting that the analyzed Ukrainian cities did not differ in high nighttime lights compared to other urban areas of the world, which caused some difficulties considering sensitivity of nighttime lights data and the research method used. It should be emphasized that although satellite monitoring data covered more than 20 years, the study used only the current/latest city boundaries. Although these results are valid only for the latitude of Ukraine, they reflect the general characteristics of the bias of widely used DMSP data on nighttime lights.

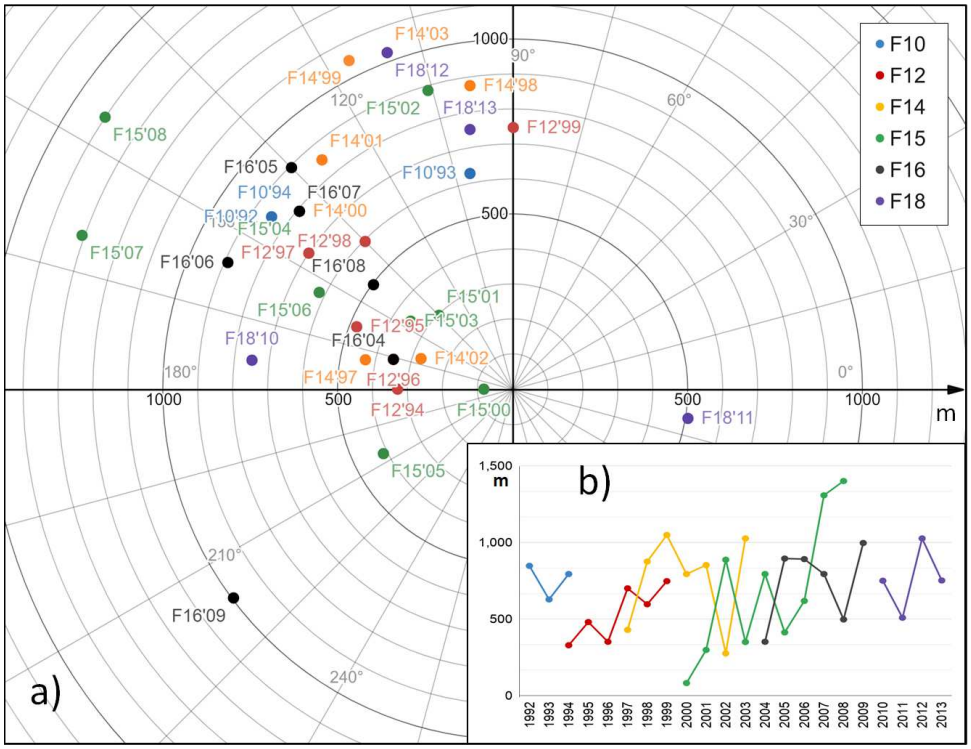

Fig. 8. Bias distance in meters and bias angle to the east in the radial coordinate system (a), and bias distance only (b) of all annual DMSP-OLS nighttime lights data composites [7]. The results were calculated after a simultaneous shift in the boundaries of 653 of the largest cities in Ukraine. DMSP satellite numbers and years of monitoring are indicated (for example, F15'08 means data from F15 satellite for 2008).

The approach presented in this article for the analysis and compensation of the ODIAC emission data bias (bias inherited from DMSP nighttime lights data bias) enables a significant reduction in the geolocation error of non-point sources of CO_2 emissions, which is very important for urban areas. As we can see from Table 1, the reduction of the geolocation error of non-point sources led to an increase in emissions within the boundaries of 17 878 cities by 4.76% (increase by 19 317 542 tC). Accordingly, emissions from non-urban areas decreased by the same amount, as the geolocation error unreasonably attributed these emissions to these areas.

[1] Yeh C., Perez A., Driscoll A., Azzari G., Tang Z., Lobell D., Ermon S., Burke M. Using publicly available satellite imagery and deep learning to understand economic well-being in Africa. Nat. Commun. **11** (1), 1–11 (2020).

[2] Lespinas F., Wang Y., Broquet G., Breon F.-M., Buchwitz M., Reuter M., Meijer Y., Loescher A., Janssens-Maenhout G., Zheng B., Ciais P. The potential of a constellation of low earth orbit satellite imagers to monitor worldwide fossil fuel CO_2 emissions from large cities and point sources. Carbon Balance and Management. **15** (1), 18 (2020).

[3] Sutton P., Dar R., Elvidge C., Kimberly B. An estimate of the global human population using night-time satellite imagery. Int. J. Remote Sens. **22** (16), 3061–3076 (2001).

[4] Bennett M. M., Smith L. C. Advances in using multitemporal night-time lights satellite imagery to detect, estimate, and monitor socioeconomic dynamics. Remote Sens. Environ. **192**, 176–197 (2017).

[5] Elvidge C. D., Baugh K. E., Kihn E. A., Kroehl H. W., Davis E. R. Mapping city lights with nighttime data from the DMSP operational linescan system. Photogramm. Eng. Rem. S. **63**, 727–734 (1997).

[6] Baugh K., Elvidge C., Ghosh T., Ziskin D. Development of a 2009 stable lights product using DMSP-OLS data. Proc. of the Asia-Pacific Advanced Network. **30**, 114–130 (2010).

[7] DMSP OLS. Nighttime Lights Time Series Version 4, Defense Meteorological Program Operational Linescan System. https://ngdc.noaa.gov/eog/dmsp/downloadV4composites.html

[8] Small C., Pozzi F., Elvidge C. D. Spatial analysis of global urban extent from DMSP-OLS night lights. Remote Sens. Environ. **96** (3–4), 277–291 (2005).

[9] Ghosh T., Anderson S. J., Elvidge C. D., Sutton P. C. Using nighttime satellite imagery as a proxy measure of human well-being. Sustainability. **5**, 4988–5019 (2013).

[10] Bruederle A., Hodler R. Nighttime lights as a proxy for human development at the local level. PLoS ONE. **13** (9), e0202231 (2018).

[11] Li L., Yu T., Zhao L., Zhan Y., Zheng F., Zhang Y., Mumtaz F., Wang C. Characteristics and trend analysis of the relationship between land surface temperature and nighttime light intensity levels over China. Infrared Phys. Techn. **97**, 381–390 (2019).

[12] Oda T., Maksyutov S. A very high-resolution (1 km × 1 km) global fossil fuel CO_2 emission inventory derived using a point source database and satellite observations of nighttime lights. Atmos. Chem. Phys. **11**, 543–556 (2011).

[13] Oda T., Maksyutov S., Andres R. J. The Open-source Data Inventory for Anthropogenic CO_2, version 2016 (ODIAC2016): a global monthly fossil fuel CO_2 gridded emissions data product for tracer transport simulations and surface flux inversions. Earth Syst. Sci. Data. **10**, 87–107 (2018).

[14] ODIAC fossil fuel emission dataset. http://db.cger.nies.go.jp/dataset/ODIAC/

[15] Chen J., Zhao F., Zeng N., Oda T. Comparing a global high-resolution downscaled fossil fuel CO_2 emission dataset to local inventory-based estimates over 14 global cities. Carbon Balance and Management. **15** (9), 1–15 (2020).

[16] Gaughan A.E., Oda T., Sorichetta A., Stevens F.R., Krauser L., Yetman G., Bun R., Bondarenko M., Nghiem S. V. Evaluation of gridded CO_2 emissions from night-time lights compared with geospatially-derived population distributions for Vietnam, Cambodia and Laos. IGARSS 2019 – 2019 IEEE International Geoscience and Remote Sensing Symposium, Yokohama, Japan, 1625–1628 (2019).

[17] Han P., Zeng N., Oda T., Lin X., Crippa M., Guan D., Janssens-Maenhout G., Ma X., Liu Z., Shan Y., Tao S., Wang H., Wang R., Wu L., Yun X., Zhang Q., Zhao F., Zheng B. Evaluating China's fossil-fuel CO_2 emissions from a comprehensive dataset of nine inventories. Atmos. Chem. Phys. **20**, 11371–11385 (2020).

[18] Oda T., Bun R., Kinakh V., Topylko P., Halushchak M., Marland G., Lauvaux T., Jonas M., Maksyutov S., Nahorski Z., Lesiv M., Danylo O., Horabik-Pyzel J. Errors and uncertainties in a gridded carbon dioxide emissions inventory. Mitig. Adapt. Strat. Gl. **24** (6), 1007–1050 (2019).

[19] Jokar Arsanjani J., Zipf A., Mooney P., Helbich M. OpenStreetMap in GIScience - Experiences, Research, and Applications. Springer (2015).

[20] Bun R., Nahorski Z., Horabik-Pyzel J., Danylo O., See L., Charkovska N., Topylko P., Halushchak M., Lesiv M., Valakh M., Kinakh V. Development of a high resolution spatial inventory of GHG emissions for Poland from stationary and mobile sources. Mitig. Adapt. Strat. Gl. **24** (6), 853–881 (2019).

[21] Charkovska N., Halushchak M., Bun R., Nahorski Z., Oda T., Jonas M., Topylko P. A high-definition spatially explicit modelling approach for national greenhouse gas emissions from industrial processes: Reducing the errors and uncertainties in global emission modelling. Mitig. Adapt. Strat. Gl. **24** (6), 941–968 (2019).

[22] Danylo O., Bun R., See L., Charkovska N. High resolution spatial distribution of greenhouse gas emissions in the residential sector. Mitig. Adapt. Strat. Gl. **24** (6), 907–939 (2019).

[23] Kinakh V., Bun R., Danylo O. Geoinformation technology for analysis and visualisation of high spatial resolution greenhouse gas emissions data using a cloud platform. Advances in Intelligent Systems and Computing II. **689**, 217–229 (2018).

[24] Crisp D., Pollock H. R., Rosenberg R., Chapsky L., Lee R. A. M., Oyafuso F. A., Frankenberg C., O'Dell C. W., Bruegge C. J., Doran G. B., Eldering A., Fisher B. M., Fu D., Gunson M. R., Mandrake L., Osterman G. B., Schwandner F. M., Sun K., Taylor T. E., Wennberg P. O., Wunch D. The on-orbit performance of the Orbiting Carbon Observatory-2 (OCO-2) instrument and its radiometrically calibrated products. Atmos. Meas. Tech. **10**, 59–81 (2017).

[25] Eldering A., Taylor T. E., O'Dell C. W., Pavlick R. The OCO-3 mission: measurement objectives and expected performance based on 1 year of simulated data. Atmos. Meas. Tech. **12**, 2341–2370 (2019).

[26] Zheng Z., Chen Y., Wu Z., Ye X., Guo G., Qian Q. The desaturation method of DMSP/OLS nighttime light data based on vector data: taking the rapidly urbanized China as an example. Int. J. Geogr. Inf. Sci. **33** (3), 431–453 (2018).

[27] de Miguel A. S., Kyba C. C., Zamorano J., Gallego J. The nature of the diffuse light near cities detected in nighttime satellite imagery. Sci. Rep. **10**, 7829 (2020).

[28] Li X., Zhou Y., Zhao M., Zhao X. A harmonized global nighttime light dataset 1992-2018. Scientific Data. **7**, 168 (2020).

[29] Letu H., Hara M., Tana G., Nishio F. A saturated light correction method for DMSP/OLS nighttime satellite imagery. IEEE T. Geosci. Remote. **50** (2), 389–396 (2012).

[30] Zhenga Q., Wenga Q., Wang K. Correcting the Pixel Blooming Effect (PiBE) of DMSP-OLS nighttime light imagery. Remote Sens. Environ. **240**, 111707 (2020).

[31] Ash K., Mazur K. Identifying and correcting signal shift in DMSP-OLS data. Remote Sens. **12** (14), 2219 (2020).

[32] Ren C., Yu Z., Deng K., Pan Y. Deblurring study of DMSP/OLS nighttime light data by RTSVD. The International Archives of the Photogrammetry, Remote Sensing and Spatial Information Sciences XLII-3/W10 (2020).

[33] Zheng Z., Yang Z., Chen Y., Wu Z., Marinello F. The interannual calibration and global nighttime light fluctuation assessment based on pixel-level linear regression analysis. Remote Sens. **11** (18), 2185 (2019).

[34] Kinakh V., Oda T., Bun R. Formulating a geolocation bias correction for DMSP nighttime lights of global cities. Advances in Intelligent Systems and Computing V. **1293**, 383–398 (2021).

Зменшення похибок геолокації супутникових даних нічного освітлення та глобальних растрових даних про емісії CO_2

Кінах В.[1], Ода Т.[2,3,4], Бунь Р.[1,5], Новіцька О.[1]

[1] *Національний університет "Львівська політехніка", вул. С. Бандери, 12, 79013, Львів, Україна*
[2] *Університети космічної дослідницької асоціації, Колумбія, МД, США*
[3] *Університет Меріленда, Коледж Парк, МД, США*
[4] *Університет Осака, Суіта, Осака, Японія*
[5] *Університет WSB, Домброва Гурніча, Польща*

Точне геопросторове моделювання емісії парникових газів (ПГ) є важливою частиною майбутньої глобальної системи моніторингу цих газів. У нашій попередній роботі було виявлено систематичний зсув у глобальних відкритих растрових даних про антропогенні емісії діоксиду вуглецю (CO_2) (ODIAC дані). Виявляється, що цей зсув зумовлений зміщенням геолокації первинних даних про нічне освітлення (NTL) супутникової програми метеорологічного моніторингу (DMSP програми), які використовуються як просторові індикатори для оцінювання розподілу неточкових джерел емісії в ODIAC. Зменшення такої похибки геолокації (~ 1.7 км), яка є того ж порядку, що і величина комірки растру супутників, що здійснюють моніторинг вуглецю, є особливо критичним для просторового аналізу емісій міст. У цій роботі запропоновано метод компенсації зміщення геолокації даних NTL DMSP, який можна застосувати до геопросторових продуктів на основі цих даних, зокрема до даних ODIAC. Для виявлення та оцінювання зміщення геолокації застосовано репозиторій OpenStreetMap, щоб визначити межі великого числа міст з усієї планети. Використано припущення, що сумарні емісії у межах міста є максимальними, якщо у NTL даних нічного освітлення відсутнє зміщення (зсув геолокації). Тому ми шукали оптимальний вектор (відстань та кут), який максимізує сумарні ODIAC емісії у містах, шляхом зміщення емісійних полів. У процесі підготовки річних композитів даних нічного освітлення деяким пікселям DMSP даних, які відповідають водним об'єктам, було присвоєно нульові значення, що із-за зміщення геолокації необґрунтовано спотворило ODIAC емісійні поля. Тому запропоновано оригінальний підхід до відновлення даних у таких пікселях, що усунуло фактор, який спотворював емісійні поля ODIAC. Розроблено також метод корекції зсувів для зміщених емісійних полів ODIAC даних високої роздільної здатності. Процедуру корекції зсувів застосовано до емісійних даних багатьох міст з різних континентів. Показано, що така корекція (усунення похибки геолокації в полях неточкових джерел емісії) збільшує сумарні емісії CO_2 у межах міст у середньому на 4.76% шляхом відповідного зменшення емісії з позаміських регіонів, куди ці емісії початково бути помилково віднесені.

Ключові слова: *дистанційне зондування, дані нічного освітлення, емісія парникових газів, зміщення супутникових даних, алгоритм аналізу зміщення.*